Available online at www.sciencedirect.com
ScienceDirect
Journal of Nuclear Materials 361 (2007) 41–51
journal of nuclear materials
www.elsevier.com/locate/jnucmat

Burnup simulations and spent fuel characteristics of ZrO_2 based inert matrix fuels

E.A. Schneider [a,1], M.R. Deinert [b,*,1], S.T. Herring [c], K.B. Cady [b]

[a] Department of Mechanical Engineering, University of Texas, Austin, TX, United States
[b] Department of Theoretical and Applied Mechanics, Cornell University, Ithaca, NY, United States
[c] Idaho National Laboratory, Idaho Falls, ID, United States

Received 18 May 2006; accepted 26 October 2006

Abstract

Reducing the inventory of long lived isotopes that are contained in spent nuclear fuel is essential for maximizing repository capacity and extending the lifetime of related storage. Because of their non-fertile matrices, inert matrix fuels (IMF's) could be an ideal vehicle for using light-water reactors to help decrease the inventory of plutonium and other transuranics (neptunium, americium, curium) that are contained within spent uranium oxide fuel (UOX). Quantifying the characteristics of spent IMF is therefore of fundamental importance to determining its effect on repository design and capacity. We consider six ZrO_2 based IMF formulations with different transuranic loadings in a 1–8 IMF to UOX pin-cell arrangement. Burnup calculations are performed using a collision probability model where transport of neutrons through space is modeled using fuel to moderator transport and escape probabilities. The lethargy dependent neutron flux is treated with a high resolution multigroup thermalization method. The results of the reactor physics model are compared to a benchmark case performed with Montebruns and indicate that the approach yields reliable results applicable to high-level analyses of spent fuel isotopics. The data generated show that a fourfold reduction in the radiological and integrated thermal output is achievable in single recycle using IMF, as compared to direct disposal of an energy equivalent spent UOX.

1. Introduction

The US inventory of civilian spent nuclear fuel is increasing at around 2000 tonnes of heavy metal each year. At present this material is destined for interment at Yucca Mountain but the opening date for the repository and its ability to isolate radiological isotopes over geological time periods are points of ongoing public and political contention [1]. Decreasing the quantity of transuranics requiring interment would reduce the long term heat and radiological loads to a repository and extend the lifetime of related storage materials. This would in turn increase a repository's capacity and make protection of the biosphere more certain. As a result, much effort has been focused on developing methods by which the long lived isotopes that are contained within spent uranium oxide fuel (SF_{UOX}) can be transmuted into more benign or shorter lived forms.

* Corresponding author.
E-mail address: mrd6@cornell.edu (M.R. Deinert).
[1] These authors contributed equally to this paper.

0022-3115/$ - see front matter © 2006 Elsevier B.V. All rights reserved.
doi:10.1016/j.jnucmat.2006.10.021

Because light-water reactors (LWR) are likely to dominate nuclear energy production in the near term, considerable interest exists in utilizing them to help reduce the large inventories of transuranics that they produce when loaded with uranium oxide fuel (UOX). At present, the only commercial-scale option for doing this is to reprocess SF_{UOX} and recycle the plutonium in mixed oxide fuel (MOX) for use in existing LWRs. However, because of neutron capture in the uranium matrix of MOX, considerable transuranics, both higher actinides and plutonium, are bred in situ even as the recycled plutonium is being fissioned. The magnitude of this effect is quantified by the conversion ratio (CR), defined as the rate of transuranic (TRU) production divided by its rate of consumption [2]. MOX fuel typically offers a conversion ratio from 0.5 to 0.7 but uranium-free fuel can function as a pure TRU burner and achieve a CR of zero. TRUs are the dominant contributors to the long term radiological load and decay heat borne by a repository and related storage materials [3]. As a result, a fuel form with a low CR would be far more efficient, per unit energy produced, at reducing the radiological inventory requiring storage as compared to either direct disposal of SF_{UOX} or TRU recycle in MOX.

In the past decade attention has been given to the use of 'inert matrix' fuels (IMFs) that would avoid the problem of the neutron capture that leads to the production of TRUs and thereby achieve a CR of zero [4,5]. In addition, it is currently envisioned that such fuels might contain not only plutonium recycled from SF_{UOX} but the other transuranics as

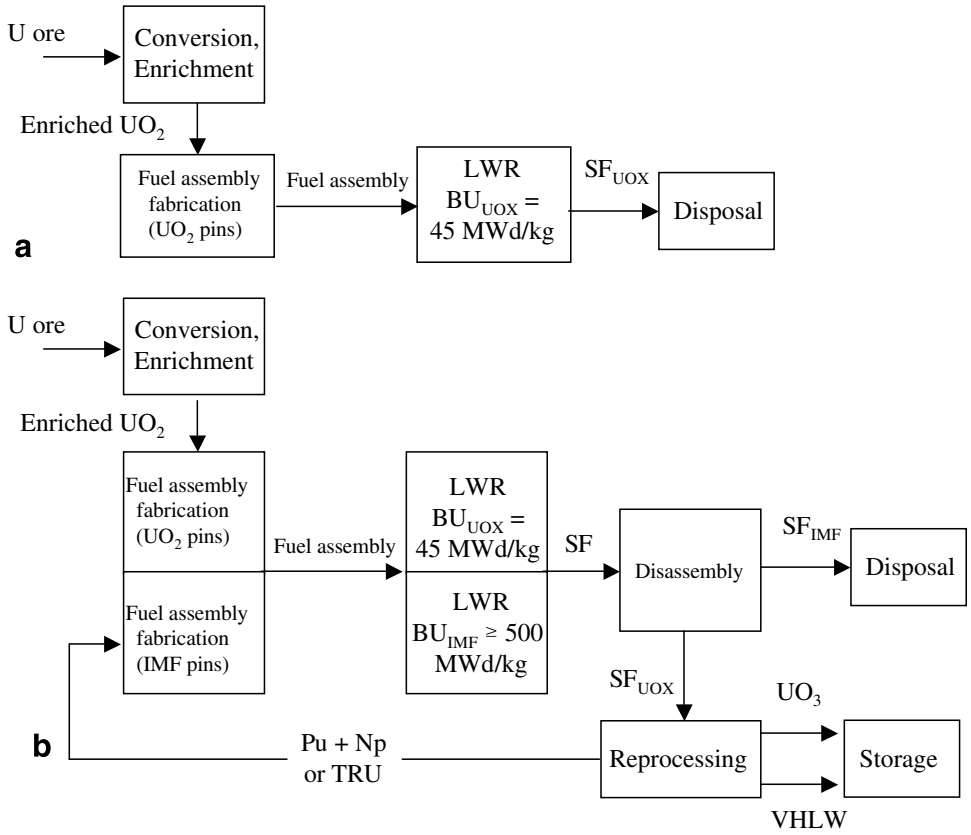

Fig. 1. Schematic of material flows for direct disposal and IMF fuel cycles: (a) Schematic of the direct disposal fuel cycle. (b) Schematic of the IMF cycle where SF_{UOX} is reprocessed to recover plutonium (along with neptunium and/or minor actinides), which is then used to make IMF and is burned and disposed of as SF_{IMF}. Connected boxes indicate locations where UOX and IMF pins are present in the same fuel assembly. UO_3 and VHLW are byproducts of this reprocessing which are stored at nominal cost. The SF_{UOX} is assumed to have a burnup of 45 MWd/kg IHM and reprocessing is assumed to occur 30 years after SF_{UOX} discharge from the reactor. IMF fabrication is assumed to occurring immediately after reprocessing with no lag between IMF fabrication and the placement of the IMF into a reactor. Note that the use of heterogeneous fuel assemblies (one pin of IMF to eight pins of UOX) requires that the IMF pins, which are not reprocessed, be separated from the UOX pins prior to reprocessing.

well (Fig. 1), making IMF particularly attractive as a means of reducing the quantity of radiological isotopes that are produced as a byproduct of LWR operation [6]. Because it is both insoluble and highly durable, yttrium stabilized ZrO_2 (YSZ) has attracted interest for this use [5,7]. Fabrication techniques are similar to those used for MOX and UOX with dry milling of constituent oxides, or co-precipitation to form a solid solution, being followed by compaction and sintering of the resulting grains [7]. Characterization of the mechanical and thermal properties of YSZ based IMF have been reported in a number of studies as has its durability under radiation bombardment. Initial results from in pile testing at the Halden test reactor (to update models for fission gas release, thermal conductivity and fuel swelling) have recently been published as well [8–10].

A number of studies have investigated the burnup and safety profiles of YSZ based IMF [4,5,11] for a single recycle system and suggest good in reactor performance. This, coupled with the potential for efficient consumption of all recycle transuranics, suggests that the use of IMF can offer benefits by decreasing the heat and radiological loads to which a repository, and related storage materials, would be subjected [12]. We expand on these previous studies and consider six YSZ and ZrO_2/MgO based IMF formulations with different weight percents of plutonium and minor actinides (Cm, Am, Np). Blends of ZrO_2/MgO have recently been suggested as a means by which the thermal conductivity of IMF could be increased, with the ZrO_2 providing protection against hydration of MgO [13]. We show here that a fourfold reduction in the radiological and integrated repository heat loads would be achievable using single recycle with high TRU loading to an IMF, as compared to direct disposal of an energy equivalent of SF_{UOX}. The primary cause of this improvement is the very high specific burnup of IMF, $\geqslant$500 MWd/kg IHM. This corresponds to the fission of more than 50% of the atoms of TRU fuel initially present. These reductions could have a dramatic benefit by extending the capacity of repositories such as Yucca Mountain.

2. Materials and methods

2.1. Overview

Burnup calculations for six IMF formulations were performed using a two region, multigroup collision probability model that has been fully benchmarked for LWRs burning UOX, MOX and IMF. The applicability of this method rests on the premise that detailed spatial variations in the neutron flux are unimportant to tracking isotope buildup and burnout provided that average cross-sections and fluxes can be derived that preserve interaction rates within macroscopic heterogeneous regions of a fuel element. Collision probability theory then models the transport of neutrons from region-to-region using transmission and escape probabilities. The overall aim is to reduce the spatial dependence of the problem to that of only a few regions. Such an approach was used in the WIMSD-5 code developed by the British [15] and was intended primarily for static neutronics calculations on thermal reactors. We have extended this approach to consider the time dependence of the spatial and energy dependent neutron flux in a reactor core in a way that is amenable to rapid computation. The concentration of 24 actinide isotopes is tracked through time (as well as fission products) and the model accepts as inputs fuel element geometry and composition, moderator/coolant geometry and composition, reactor geometry, fuel residence time and fuel discharge burnup.

The implementation of the reactor physics model (VBUDS: visualization, burnup, depletion and spectrum) uses collision probability approximations to the neutron transport equation to decouple the spatial and energy variables. The lethargy dependent neutron flux, governed by coupled integral equations for the fuel and moderator/coolant regions is treated by multigroup thermalization methods, and the transport of neutrons through space is modeled by fuel-to-moderator transport and escape probabilities. The transport equation is formulated as a set of coupled integral equations in energy. To reduce the problem of solving these, the spatial and energy variables are decoupled and the isotropic and linearly anisotropic components of the elastic scattering kernel in the center-of-mass system are preserved.

To model the transport of neutrons between the spatial regions in the fuel and moderator/coolant, an effective cell consisting of a homogeneous fuel element surrounded by a region of homogeneous moderator/coolant is constructed. The spatial dependence of the flux is treated by taking the neutron number density in the respective fuel and moderator/coolant regions to be uniform. This simplification greatly facilitates spatial transport

computations, as it allows us to apply the reciprocity theorem. The movement of neutrons between regions is then governed by transmission and escape probabilities, which are themselves functions of energy. It is important to emphasize that the goal is not to accurately model the spatial dependence of the flux, but instead its spectral dependence and through this the time dependent concentration of isotopes in the reactor as a whole.

VBUDS uses a multigroup formulation to treat neutron energy dependence. The ENDF/B-VI data were processed using NJOY99 to yield cross-section libraries at five temperatures (300, 600, 900, 1200, 1500 K). Cross-sections come bundled with VBUDS for a wide range of potential constituents which include the 24 actinide isotopes, oxide, nitride, zirconia, and zirconium hydride fuel forms, common cladding and structural materials (e.g., Zircaloy, HT-9), control absorbers (boron, B_4C, Ag–In–Cd, Gd_2O_3) and a number of common moderators and coolants (light- or heavy-water, graphite, helium, CO_2, lead, bismuth and sodium). Rather than adopt any of the currently existing energy meshes, we use an energy grid in which all bins are of equal lethargy width. This mesh, which contains 10 (coarse representation) or 100 (fine) bins per neutron energy decade, was chosen because the set of nucleides whose resonances might determine the binning structure could vary widely between VBUDS runs.

To date VBUDS has been fully tested against LWR, UOX and MOX benchmarks that are available from the NEA/OECD [16,17] and against IMF burnup calculations that were done using Monteburns, all with strong fidelity, see Section 2.3.

2.2. Relative cumulative decay heat and radioactivity

The output from the VBUDS simulations was used in conjunction with the ORIGEN2.2 [18] database of isotope properties to determine the time dependent radioactivity and cumulative decay heat [Watt-years] for SF_{IMF} from the individual cases (see next section). We choose SF_{UOX} with a burnup (BU_{UOX}) of 45 MWd/kg IHM as a basis for comparison, as well as a TRU source from which IMF will be made. The relative performance measures (radioactivity and cumulative decay heat) for IMF versus direct disposal cycles are calculated on an energy equivalent basis as follows. Let x[kg IHM] be the amount of IMF fuel that can be made from the TRU's contained in 1 kg of SF_{UOX}. The burnup achieved by this IMF, BU_{IMF} [MWd/kg IHM] is computed using VBUDS. The total energy released from the IMF during its burn plus the energy produced by irradiation of the initial 1 kg of UOX is

$$E = \mathrm{BU}_{\mathrm{UOX}} + x\mathrm{BU}_{\mathrm{IMF}}. \quad (1)$$

Producing this amount of energy using a once-through UOX cycle would require y kg IHM of UOX with:

$$y = E/\mathrm{BU}_{\mathrm{UOX}}. \quad (2)$$

The relative integrated decay heat and radioactivity of the IMF cycle are then obtained by dividing the outputs from 1 kg $SF_{UOX} + x$ kg SF_{IMF}, by the respective outputs from y kg SF_{UOX}.

2.3. IMF case specification

Tables 1–4 specify both the type of the inert matrix to be investigated as well as the initial isotopic composition of the fuel. Two IMF matrices were considered, YSZ with 92 w/o Y_2O_3–8 w/o ZrO_2 and $MgOZrO_2$ with 40 w/o MgO–60 w/o ZrO_2, where w/o denotes 'weight percent'. The cycle parameters are taken from Herring et al. [6], except for the temperatures and water density typical of a PWR taken which are taken from the BU credit benchmark, Vol IV-B [17]. An infinite lattice is assumed in all cases.

Discharge burnups were determined in the usual manner for pin-cell, pin array, or fuel assembly level calculations. The infinite medium multiplication factor, k_∞, was computed as a function of fuel burnup with leakage taken into consideration through a non-leakage probability, P_{NL}, such that $k_{eff} = k_\infty P_{NL}$. For a three-batch reloading scheme, k_{eff} was then determined for each fuel batch at the conclusion of each irradiation period. The discharge burnup was defined as that burnup for which k_{eff}

Table 1
Specification of IMF burnup cases

Matrix for inert matrix fuels (w/o)				
Case	Matrix		Fuel	
	$YstabZrO_2$	$MgOZrO_2$	Pu + Np	TRU
1	92		8	
2	92			8
3		92	8	
4		92		8
5		88	12	
6		85		15

Here 'Stab' stands for stabilized, TRU for all transuranics and 'w/o' for weight percent.

Table 2
Input isotopic composition of the Np and Pu used cases 1, 3, 5 and 'a/o' stands for atom percent

Isotope	Fraction of Pu + Np (a/o)	Isotope fraction (a/o)
Np-237	6.9	100.0
Pu-238	2.0	2.2
Pu-239	55.9	60.0
Pu-240	24.8	26.6
Pu-241	3.6	4.0
Pu-242	6.7	7.2

Table 3
Input isotopic composition of TRU used in cases 2, 4, 6 and 'a/o' stands for atom percent

Isotope	Fraction of TRU (a/o)	Isotope fraction (a/o)
Np-237	6.0	100.0
Pu-238	1.8	2.2
Pu-239	49.0	60.0
Pu-240	21.7	26.6
Pu-241	3.3	4.0
Pu-242	5.9	7.2
Am-241	10.8	89.1
Am-242m	0.0	0.1
Am-243	1.3	10.9
Cm-242	0.0	0.0
Cm-243	0.0	1.7
Cm-244	0.2	84.7
Cm-245	0.0	11.9
Cm-246	0.0	1.6

equaled one. This approach, though elementary, has found wide use [19] and we have adopted it here.

To capture the heterogeneous nature of the fuel loading, k_{eff} was determined as a function of fuel burnup, and burnup as a function of fluence, for both IMF and UOX pin-cells. Assuming that the fluences in the IMF and UOX cells were the same, a k_{eff} versus burnup profile was then assembled for the 1:8 IMF-to-UOX lattice as a weighted average of the two. This approach was found to yield good results, see below, but would not be applicable to extreme lattice heterogeneities such as burnable targets.

A detailed description of k_{∞} and P_{NL} calculations in VBUDS can be found in [14].

2.4. Benchmark

We consider an inert matrix fuel with 92 w/o zirconium oxide and 8 w/o transuranics (case 2 above) where one of nine pins in a pin-cell configuration is IMF. The vector for the TRU is given in Table 4. We use VBUBS to calculate the beginning and end of life neutron spectra for the core, the time dependent neutron production rates for 24 actinides and parameters for the six factor formula (reproduction factor, thermal utilization factor, k_{eff}, etc.) as a function of fuel burnup. The results are obtained by using a weighted average from simulations done on full IMF and UOX pin-cell configurations. Isotope buildup and burnout for this case were also simulated using Monteburns to provide a point of comparison to VBUDS calculations.

3. Results

Figs. 2 and 3 show representative isotopic concentrations during burnup for case 2 simulations

Table 4
Initial and final actinide concentrations for the IMF in cases 1–3, given in weight percent of IHM

Isotope	Case 1		Case 2		Case 3	
	Initial	Final	Initial	Final	Initial	Final
Np-237	6.87	2.28	6.03	2.05	6.87	2.94
Pu-238	2.01	3.22	1.81	5.92	2.01	3.38
Pu-239	55.85	1.24	48.63	1.86	55.86	2.02
Pu-240	24.77	8.70	21.83	7.84	24.77	11.96
Pu-241	3.75	4.36	3.32	4.09	3.75	5.72
Pu-242	6.74	10.70	5.94	10.55	6.74	10.34
Am-241	0	0.239	10.87	0.609	0	0.381
Am-242m	0	0.005	0	0.012	0	0.007
Am-243	0	2.46	1.31	2.91	0	2.27
Cm-242	0	0.248	0	0.789	0	0.242
Cm-243	0	0.007	0.005	0.034	0	0.006
Cm-244	0	1.67	0.232	2.52	0	1.19
Cm-245	0	0.079	0.033	0.126	0	0.055
Cm-246	0	0.030	0.004	0.068	0	0.015

The burnup for case 1 was BU 585 (MWd/kg IHM), for case 2 it is 550 (MWd/kg IHM), and for case 3 it is 540 (MWd/kg IHM).

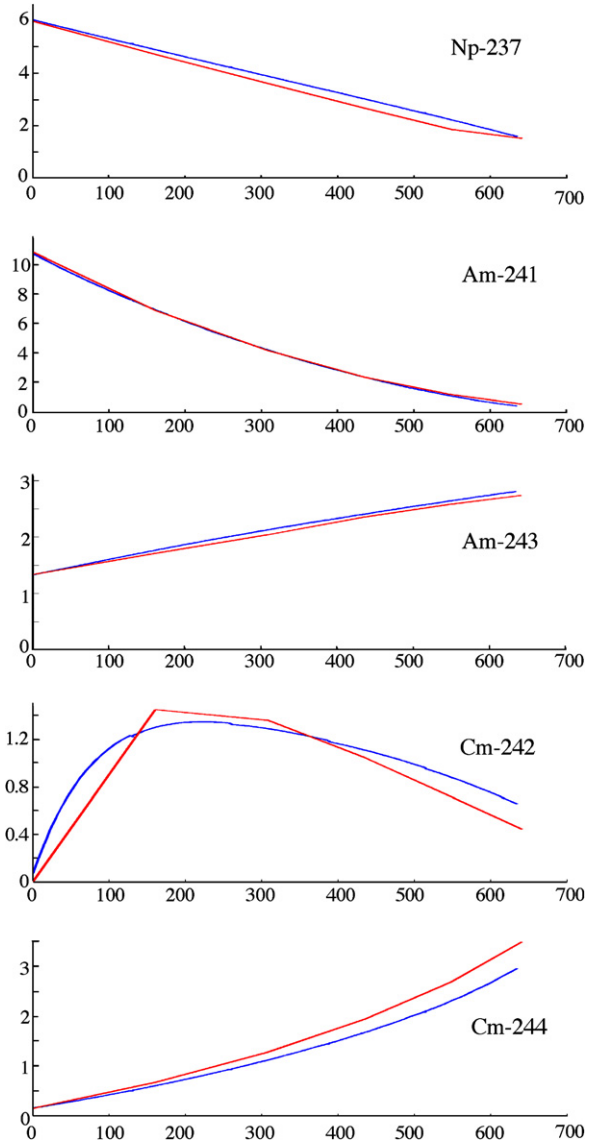

Fig. 2. Benchmark of Am and Cm isotopes predicted by VBUDS and Monteburns. The prevalence of Np-237, Am-241, Am-243, Cm-242, Cm 244 as a function of burnup as predicted by VBUDS (blue) and Monteburns (red). Horizontal axes are burnup (MWd/kg IHM) and the vertical axes are percent of initial heavy metal (% IHM). The benchmark case considered a pin of IMF in a nine pin assembly where the IMF was a Y stabilized ZrO_2 with 8 w/o Pu + MA and a Pu and MA vector as specified in Herring et al. [6]. (For interpretation of the references in color in this figure legend, the reader is referred to the web version of this article.)

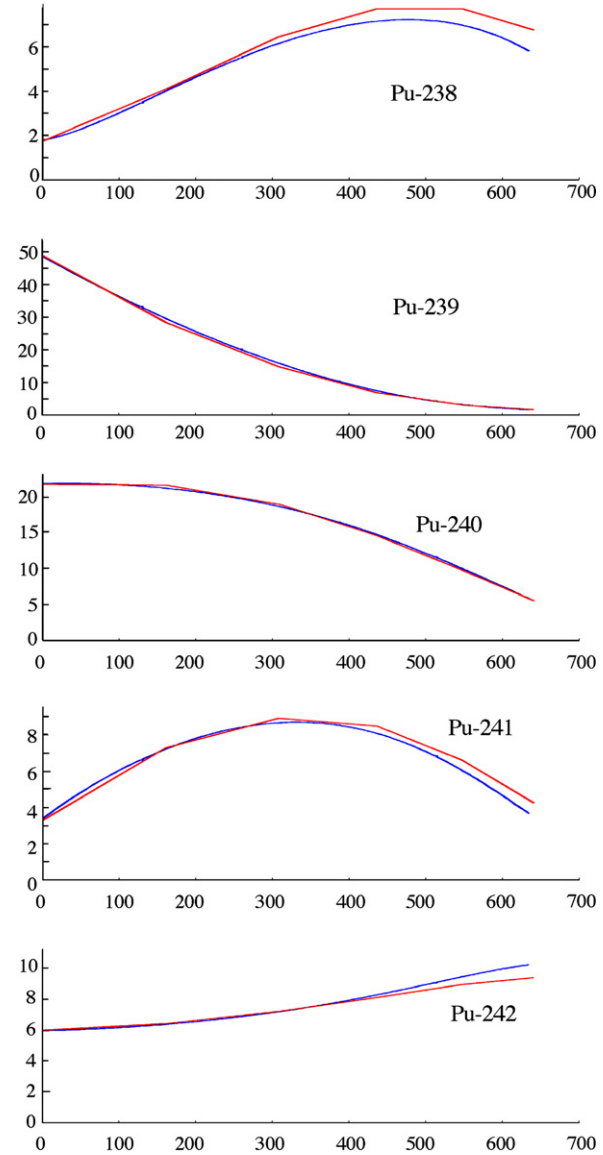

Fig. 3. Benchmark of Pu isotopes predicted by VBUDS and Monteburns. The prevalence of Pu-238–Pu-242 as a function of burnup as predicted by VBUDS (blue) and Monteburns (red). Horizontal axes are burnup (MWd/kg IHM) and the vertical axes are percent of initial heavy metal (% IHM). The benchmark case considered a pin of IMF in a nine pin assembly where the IMF was a Y stabilized ZrO_2 with 8 w/o Pu + MA and a Pu and MA vector as specified in Herring et al. [6]. (For interpretation of the references in color in this figure legend, the reader is referred to the web version of this article.)

done with VBUDS and Monteburns. The correlations are in line with previous results that compared VBUDS simulations of uniform core loadings of MOX and UOX in LWRs to OECD benchmarks. While the IMF pin-cell configurations represent inhomogeneous LWR core loadings the method of using a weighted average of VBUDS simulations for uniform IMF and UOX loadings, as described above, gives results that correlate well with those generated using Monteburns. This is likely due to the relatively short neutron mean free path in an

Table 5
Initial and final actinide concentrations for the IMF in cases 4–6, given in weight percent of IHM

Isotope	Case 4		Case 5		Case 6	
	Initial	Final	Initial	Final	Initial	Final
Np-237	5.99	2.61	6.87	1.50	5.99	0.945
Pu-238	1.80	6.41	2.01	2.60	1.80	3.81
Pu-239	48.95	2.60	55.85	0.721	48.95	1.01
Pu-240	21.69	10.55	24.77	4.63	21.69	3.03
Pu-241	3.30	5.27	3.75	2.41	3.30	1.72
Pu-242	5.90	10.21	6.74	10.88	5.90	10.14
Am-241	10.80	1.12	0	0.092	10.80	0.093
Am-242m	0	0.023	0	0.002	0	0.002
Am-243	1.30	2.83	0	2.70	1.30	2.85
Cm-242	0	0.879	0	0.229	0	0.510
Cm-243	0.005	0.033	0	0.008	0.005	0.024
Cm-244	0.231	2.00	0	2.48	0.230	3.88
Cm-245	0.032	0.102	0	0.099	0.032	0.157
Cm-246	0.004	0.043	0	0.065	0.004	0.162

The burnup for case 4 is 500 (MWd/kg IHM), for cases 5 and 6 it is 650 (MWd/kg IHM).

LWR (which servers to somewhat isolate pins from their neighbors) and the fact that the IMF pins considered here are not unlike their UOX counterparts in terms their flux spectrum. The very strong correlations shown in Figs. 2 and 3, along with the previous LWR benchmarks, confirm the applicability of VBUDS for LWR burnup simulations for a variety of fuel types, including the present ones.

Tables 4 and 5 give the charge and discharge actinide compositions of the IMF in units of weight percent of initial heavy metal (IHM). In all cases Pu-239 consumption of more than 95% was achieved, which is consistent with previous studies [4,5]. As would be expected, the high plutonium loading cases (5 and 6) achieved the greatest consumption rates with just under and over 98%, respectively. These results indicate that the high burnup offered by IMF would be particularly effective at disposing of weapons grade plutonium. In general, the presence of the other transuranics (Am, Cm) in the fresh IMF decreased the degree of plutonium burn somewhat, which would be expected because of their effect upon the neutron balance. The overall consumption of plutonium ranged from 57% (case 4) to 77% and 76% for cases 5 and 6, respectively. The consumption of neptunium ranged from a low of 56 to a high 85% for cases 4 and 6, respectively. A greater than 90% consumption of Am-241 was observed in the cases with full TRU loading with consumption of total Am ranging from 67% to 75% for cases 4 and 6, respectively. Both neptunium and americium consumption increased with increasing burnups. In all cases a net positive curium buildup is observed, though net curium production per unit energy decreases for cases where all transuranics are retained in the IMF as well as for fuel configurations achieving higher discharge burnup. It should be noted that the while the discharge burnup of the IMF was chosen to meet core-average reactivity constraints, the degree of burn could be adjusted by modifying the UOX enrichment in assemblies where IMF is present. Therefore, to maximize the transmutation potential of IMF, the fuel loading would be configured such that IMF pins would function, late in their burnup cycle, as targets supported by neighboring UOX pins. The maximum TRU burnup fraction that can be achieved through such a strategy has not yet been assessed and will be the subject of future work.

Table 6 shows the benefit in reducing transuranic heat load and radioactivity by reprocessing SF_{UOX} and recycling some or all transuranics in IMF's. The benefit or savings factor is given, by case, for a fuel cycle with single recycle through IMF as compared to direct disposal of an energy equivalent of SF_{UOX}. As can been seen, the cases where all TRUs are included in the IMF offer the greatest savings in radiological and integrated heat loading. This indicates that partitioning and storage of the unrecycled TRUs (Am, Cm) is disadvantageous for IMF strategies that are intended to enhance repository capacity, a result that is not observed with MOX. Case 6 offers the most profound savings relative to direct disposal and indicates that a four fold reduction in integrated heat load could be achieved at 1500 years after emplacement, which is considered to be a

Table 6
Relative heat and radiological outputs of IMF vs direct disposal

Case	100 year decay power	1000 year decay power	100–1500 year cumulative decay heat	10 000 year activity
1	0.82	0.59	0.67	0.32
2	0.88	0.31	0.45	0.34
3	0.94	0.73	0.82	0.37
4	0.99	0.39	0.54	0.38
5	0.75	0.55	0.63	0.28
6	0.56	0.17	0.24	0.26

The table shows the relative decay power, cumulative decay heat and radioactivity for an IMF cycle as compared to direct disposal of an equivalent of UOX. The results are computed by considering only the transuranic actinides within the IMF as well as their decay daughters. Fission products that are separated during reprocessing are assumed to be left out of a repository and, hence, would have no effect on it. However, it can be shown that these fission products have a negligible effect on the results. The integrated decay heat for SF_{IMF} is that which occurs between 100 and 1500 years after IMF discharge from a reactor.

limiting factor in determining the capacity of Yucca Mountain [20]. A similar decrease is seen for the radiological load at ten thousand years after emplacement. Such reductions could translate into a significant increase in repository capacity.

Each of the transuranic isotopes found in SF_{UOX} and SF_{IMF} is a member of one of the four actinide decay chains, Tables 7 and 8 and Figs. 4 and 5. Three of these chains, 4N, 4N + 2 and 4N + 3 contain naturally occurring radioisotopes (^{232}Th, ^{238}U and ^{235}U, respectively). The only way for a species to leave the decay chain of which it is a member is for it to capture a neutron or to fission, and IMF transmutation gives recycled actinides a second chance at both. Once spent fuel is discharged from a reactor and slated for disposal, the mass and constituency of each decay chain is fixed forever. While the initial distribution of the isotopes in the respective decay chains of course varies between IMF and UOX SF, the species that dominate the heat production and activity within each are the same.

In the very long term, the longest lived daughter in each actinide decay chain will dominate, and the activity or heat load for the chain will be governed by how much of this species is present, which is in turn determined by how many atoms were initially present in each decay chain. Figs. 4 and 5 underscore the reductions in radiological and thermal outputs for case 6 relative to an energy equivalent of UOX. The figures show a significant decrease in both thermal and radiological output for the IMF cycle relative to the UOX option. The actinide mass

Table 7
The half lives (year) of long-lived ($T_{1/2} > 0.1$ year) isotopes are shown

Z\A	4N + 1	4N + 2	4N + 3	4N	4N + 1	4N + 2	4N + 3	4N	4N + 1	4N + 2
	237	238	239	240	241	242	243	244	245	246
(96)Cm						0.45	2.91	18.1	8.50E3	4.76E3
(95)Am					433	1140	7.40E3			
(94)Pu		87.7	2.40E4	6.56E3	14.4	3.75E5				
(93)Np	2.14E6									

Since almost all nuclides undergo α and/or β decay exclusively, the decay daughters of a nuclide lie within the same decay chain as the parent.

Table 8
Actinide decay chains and the effects on UOX and IMF cycles

Decay chain	Effects
4N	Dominates medium (1–10 k) year radioactivity and for long (>1000 year) term decay power in SF_{UOX}. For the discharged IMF of case 6, it is reduced, on an energy equivalent basis, by 73%
4N + 1	Dominates short (<1e3 year) and very long term (>1e6 year) radioactivity. It's also a major contributor to medium (100–1000 year) decay power. IMF case 6 reduces the inventory of this chain by 88%
4N + 2	Is a major contributor to long (1e5–1e6 year) term radioactivity. It also influences short-medium term (50–300 year) decay power. IMF case 6 increases the inventory of this chain by 60%
4N + 3	Is a significant contributor to medium to long term (5e3–5e5 year) radioactivity in UOX SF. It also plays a major role in driving the long (>1000 year) term decay power. IMF case 6 decreases the inventory of this chain by 93%

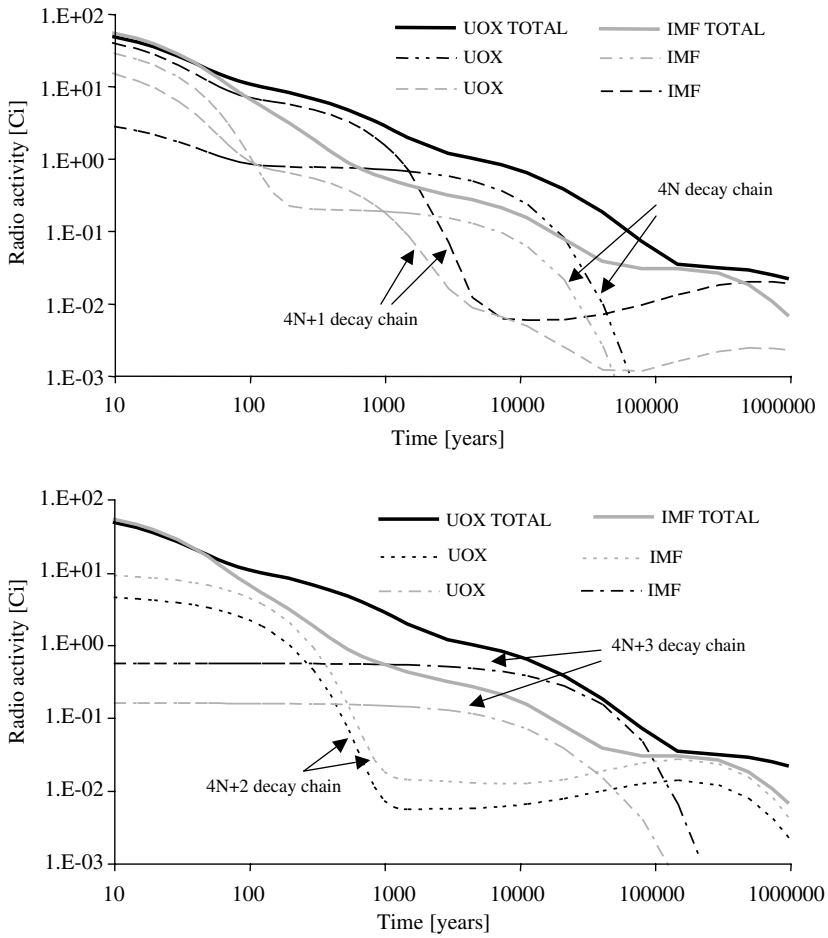

Fig. 4. Radioactivity from IMF and UOX cycles. Radioactivity from SF_{IMF} (case 6) and an energy equivalent of SFUOX are shown. Here 1 kg of SF_{UOX} is burned to 45MWd/kg HM and the resulting SFUOX is reprocessed to give 0.013 kg of IMF which is itself burned and disposed of as SF_{IMF}. An energy equivalent of UOX, with a 45 MWd/kg IHM burnup, is 1.19 kg. Overall, the actinide mass requiring long term storage is decreased by 73% for the chain 4N, 88% for 4N + 1 and 93% for 4N + 3. The IMF option gives a significant reduction in radiological output over the majority of the time course shown.

requiring long term storage is reduced for all decay chains except 4N + 2. Table 8 summarizes the effect of each of the respective actinide decay chains and how and IMF cycle effects them.

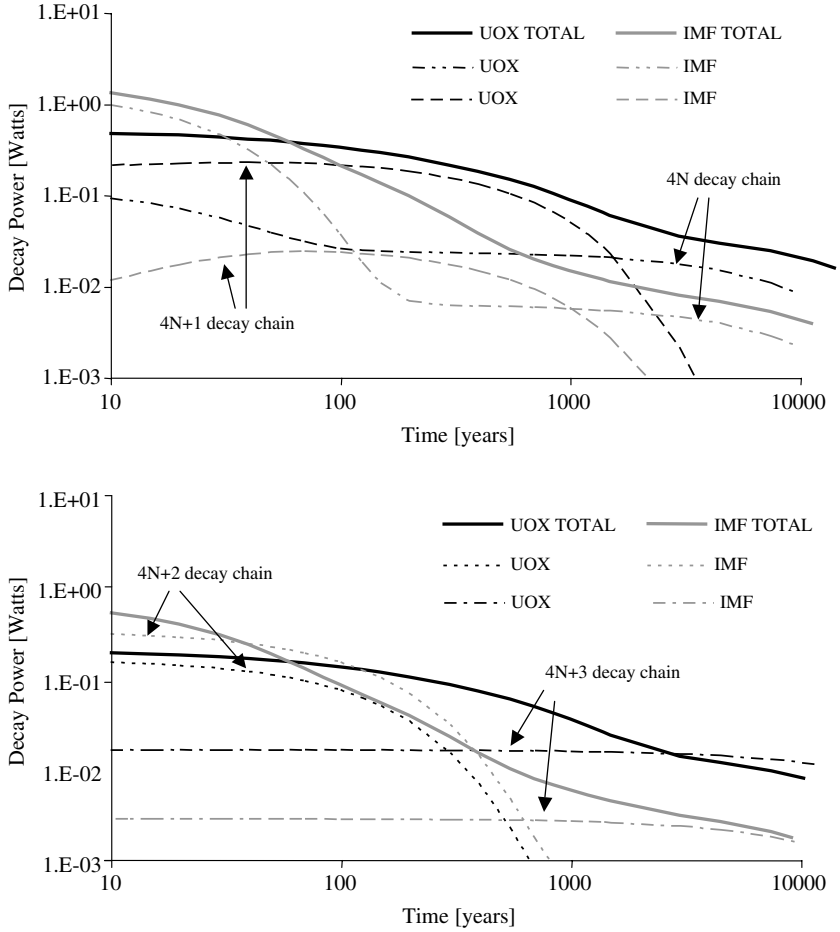

Fig. 5. Decay power from IMF and UOX cycles. Decay power from SF_{IMF} plus the VHLW from reprocessing (case 6) and an energy equivalent of SF_{UOX} are shown. The IMF option gives a fourfold reduction in integrated thermal output at 1500 years and beyond.

For moderate (a few hundred MWd/kg) burnups, the higher the IMF burnup, the more pronounced the burnout of other decay chains (and buildup of $4N + 2$ isotopes) becomes. However, case 6 reaches a sufficiently high burnup for even the $4N + 2$ membership to reach a peak and begin to be consumed. Chain $4N + 2$ is in addition relatively innocuous, as in the long term its members decay to uranium-238. Therefore, concentration of the actinides in the chain $4N + 2$ results in benefits to performance indicators outweighing the buildup of these isotopes. The benefits are less pronounced in those specific areas where members of the $4N + 2$ chain do play a significant role in driving heat load and activity, as outlined above. Additionally, if the IMF burnup could be increased further, even the mass in this decay chain could be reduced and this will be the subject of future work.

Previous studies have investigated the safety profile of ZrO_2 based IMF with plutonium loadings similar to those in cases 5 and 6 and suggest that use of such fuel would be possible [5]. While the simulations for cases 5 and 6 were for MgO/ZrO_2 blends, the isotopic profile at end of life would be nearly identical for a pure YSZ based IMF, with equivalent TRU loading, as both Mg and Zr are highly transparent to thermal neutrons. This is significant as considerable work has already gone into assessing the usability of YSZ based IMF in LWRs.

4. Conclusions

- ZrO_2 based IMF's can achieve a more than 95% consumption of Pu-239 and up to a 77% overall reduction in plutonium if a high fuel burnup can be achieved.

- Consumption of Am-241 of over 90% is achievable with ZrO_2 based IMF's and overall americium consumptions of more than 67–75% can be achieved when all TRUs are recycled and is burnup dependent. Consumption of Np-237 of up to 85% was observed in simulations of IMF at burnups of 650 Mwd/kg IHM. The curium content of IMF is seen to increase over its lifetime in the core, though the rate of increase is less when all TRUs are recycled in the IMF.
- A fourfold reduction in the radiological and integrated heat loads can be achieved with high burnup ZrO_2 based IMF, as compared to direct disposal of SF_{UOX} on a per kW h basis. This reduction can offer significant increases in repository capacity and reductions in radiological load.
- Comparison of the results of the reactor physics model to those from benchmark case generated using Monteburns indicates that VBUDS yields reliable results applicable to high-level analyses of spent fuel isotopics.

Acknowledgment

This work was supported with funds from INL Contract #00044294.

References

[1] Z.W. Xu, M.S. Kazimi, M.J. Driscoll, Nucl. Sci. Eng. 151 (2005) 261.
[2] J.R. Lamarsh, Introduction to Nuclear Reactor Theory, Addison Wesley Publishing Company, Reading, MA, 1972.
[3] S. Piet, B. Dixon, R. Hill, E.A. Schneider, D. Shropshire, J.D. Smith, R. Wigeland, Objectives, strategies and challenges for the advanced fuel cycle initiative, in: Proceedings of the American Institute of Chemical Engineering, Atlanta GA, 2005.
[4] C. Lombardi, A. Mazzola, Ann. Nucl. Energy 23 (1996) 1117.
[5] U. Kasemeyer, J.M. Paratte, P. Grimm, R. Chawla, Nucl. Technol. 122 (1998) 52.
[6] J.S. Herring, P.E. MacDonald, K.D. Weaver, Nucl. Technol. 147 (2004) 84.
[7] G. Ledergerber, C. Degueldre, P. Heimgartner, M.A. Pouchon, U. Kasemeyer, Prog. Nucl. Energy 38 (2001) 301.
[8] C. Degueldre, C. Hellwig, J. Nucl. Mater. 320 (2003) 96.
[9] C. Hellwig, M. Pouchon, R. Restani, F. Ingold, G. Bart, J. Nucl. Mater. 340 (2005) 163.
[10] C. Hellwig, U. Kasemeyer, J. Nucl. Mater. 319 (2003) 87.
[11] U. Kasemeyer, C. Hellwig, J. Lebenhaft, R. Chawla, J. Nucl. Mater. 319 (2003) 142.
[12] B. Richter, D.C. Hoffman, S.K. Mtingwa, R.P. Omberg, S. Pillon, J.L. Rempe, Report of the Advanced Nuclear Transformation Technology Subcommittee of the Nuclear Energy Research Advisory Committee, Department of Energy, Washington DC, 2002.
[13] P.G. Medvedev, S.M. Frank, T.P. O'Holleran, M.K. Meyer, J. Nucl. Mater. 342 (2005) 48.
[14] E.A. Schneider, M.R. Deinert, K.B. Cady, J. Nucl. Mater. 357 (2006) 19.
[15] A.T. Answers Software Service, WIMSD A Neutronics Code for Standard Lattice Physics Analysis, OECD/NEA, Winfrith, United Kingdom, NEA-1507/02, June 1997.
[16] M. Takano, Burnup credit criticality benchmark – result of phase 1A, NEA, NEA/NSC/DOC (93) 22, 1994.
[17] G.J. O'connor, Burnup criticality benchmark – phase IV-B: results and analysis of MOX fuel depletion calculations, NEA/OECD, 2003, ISBN 92-64-02124-8.
[18] A.G. Croff, A users manual for the ORIGIN2 computer code, Oak Ridge National Laboratory, Oak Ridge TN, ORNL/TM-7175, July 1980.
[19] M.J. Driscoll, T.J. Downar, E. Pilat, The Linear Reactivity Model for Nuclear Fuel Management, American Nuclear Press, La Grange Park, IL, 1990.
[20] DOE, The path to sustainable nuclear energy, basic and applied research opportunities for advanced fuel cycles, Department of Energy, Washington DC, September 2005.